

LOCAL VERSUS GLOBAL DECARBURIZATION DURING HYDROGEN ATTACK IN A VESSEL

S.M. Schlögl and E. van der Giessen *

One of the dangerous failure modes of pressure vessels filled with hydrogen, such as in the petrochemical industry, is by hydrogen attack. During this process, the dissolved hydrogen reacts with the carbon of the steel to form methane in grain boundary cavities. This leads to progressive development of damage inside the material, but at the same time to a decrease of the carbon content in the steel. This reduction depends, among other factors, on the methane pressure and the damage state. As the carbon content also effects the creep parameters, this process of decarburization may have an effect on the failure time. A micromechanically based continuum damage model is presented to estimate the decarburization across the wall thickness of vessels made of 2.25Cr-1Mo steels with different microstructures and its effects on the hydrogen attack life-time.

INTRODUCTION

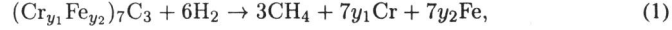
Hydrogen attack (HA) is a material degradation process occurring in steels exposed to high pressures of hydrogen at elevated temperatures. These conditions often occur in the petrochemical industry, for example in reactors for hydrocracking, hydrotreating and similar refinery applications. Inside such a component, the small hydrogen atoms can easily diffuse into the vessel wall. There, they react with the carbon of the steel to form methane. Cavities filled with methane grow at grain boundaries, and cavity coalescence leads to microcracks and intergranular failure, similar to creep rupture.

The supply of carbon for the chemical reaction to methane taking place inside the cavities occurs by a complex physico-chemical process. Depending on the actual composition and temperature, carbon may be delivered predominantly by the grain boundary carbides (local decarburization) or may be also provided by the matrix. If carbon diffusion is fast, decarburization of the matrix will take place (global decarburization) which may change the creep properties significantly and, as a consequence of that, the hydrogen attack evolution. In this paper, a micromechanically-based continuum damage model is presented to study the effect of global decarburization on the hydrogen attack failure of a pressure vessel made of 2.25Cr-1Mo steel.

*Micromechanics of Materials Group, Delft University of Technology, The Netherlands.

DECARBURIZATION

2.25Cr-1Mo is a common material for a pressure vessel. This bainitic steel consists of a ferritic matrix and alloy carbides. Their crystal structure (M_3C , M_7C_3 , $M_{23}C_6$) and composition depend on the alloy composition and the heat treatment. During hydrogen attack these carbides can react with the dissolved hydrogen to form methane. We write down this reaction for the most important carbide M_7C_3 as



where y_1 and y_2 are the concentration parameters of Cr and Fe, respectively ($y_1 + y_2 = 1$).

Cavities nucleate at the grain boundaries and they are filled with methane and hydrogen. We assume that the chemical reaction (1) reaches its equilibrium quickly as compared to the total lifetime. The partial equilibrium methane pressure p_{CH_4} in a cavity is calculated with the thermodynamical relations described in [1]. These relations also take into account the non-ideality of the methane gas. They are based on approximate solutions of the equation of state for methane [2]

$$Z(p_{CH_4}, T) = 1 + C(T)p_{CH_4} = \frac{p_{CH_4}V_m}{RT}, \quad (2)$$

where $Z(p_{CH_4}, T)$ is the molar compressibility and V_m the volume of one mole of methane. The temperature-dependent coefficient $C(T)$ for methane is also given in [2].

Sufficiently many carbon atoms have to react with the hydrogen atoms to build up the partial equilibrium pressure p_{CH_4} in a cavity. The necessary amount of carbon per cavity, n_c^{cav} , is related to the volume of the cavity, V^{cav} , by $n_c^{cav} = V^{cav}/V_m$ [mol]. Its mass m_c^{cav} is equal to $n_c^{cav}M_c$ with M_c the molecular weight of carbon. Using equation (2), we can calculate m_c^{cav} as follows

$$m_c^{cav} = \frac{p_{CH_4}V^{cav}M_c}{RT(1 + C(T)p_{CH_4})}. \quad (3)$$

When global decarburization takes place, this amount of carbon originates from the steel. Some carbides at and near the grain boundaries dissolve and "their" carbon atoms diffuse through the matrix to the cavities to react with the hydrogen. The change in carbon concentration will be (partly) compensated by transport of carbon from the matrix. Therefore, the carbon content around a cavity decreases and so does the average carbon content of the grains. Before the steel is attacked by the hydrogen, a grain occupying a volume V_g and total mass $m^0 = \rho V_g$ contains a certain mass of carbon, m_c^0 , determined by the steel composition c : $m_c^0 = \rho c^0 V_g$ (ρ is mass density, c^0 the initial carbon content of the steel). If the grain is attacked uniformly along its facets, the number of cavities, N^{cav} , is the same on all facets and all cavities belonging to this grain have the same volume V^{cav} and the same methane pressure p_{CH_4} . The mass of the carbon atoms that have to diffuse from the grain to its facets to build up the methane pressure there, is equal to $m_c^n = \frac{1}{2}N^{cav}m_c^{cav}$. Therefore, the average carbon content c_c of a uniformly attacked grain decreases to

$$c_c = \frac{m_c^0 - m_c^n}{m^0 - m_c^n} = \frac{\rho c^0 V_g - \frac{1}{2}N^{cav}m_c^{cav}}{\rho V_g - \frac{1}{2}N^{cav}m_c^{cav}}. \quad (4)$$

Equation (4) together with equation (3) show how methane pressure p_{CH_4} and cavity volume V^{cav} determine the average carbon content of a grain. Inside the vessel, the hydrogen pressure p_{H_2} is a function of the radius: $p_{H_2,i}$ at the inner wall and $p_{H_2,o} = 0$ at the outside. The cavity volume is partly controlled by the methane pressure (the governing evolution equations will be briefly summarized in the next section). Therefore, the equilibrium methane pressure, the damage and the carbon content will vary over the wall thickness. The distribution of the carbon content can be calculated with the equations (4) and (3) under the assumption that the carbon atoms diffuse over distances comparable to the grain size and not over distances on the scale of the wall thickness.

Since the carbon content effects the creep properties of a 2.25Cr-1Mo steel [3], the model for hydrogen attack in a vessel has to account for creep parameters that are coupled to the damage evolution. This means that the creep parameters in an attacked vessel have to be updated for each position in the wall.

DAMAGE MODEL

Space limitations prevent us from giving details of the model for hydrogen attack damage development; they may be found in [4, 5]. It suffices to outline here the key characteristics.

The model entails a macroscopic description of hydrogen attack damage in a material that would exhibit isotropic thermoelasticity and isotropic creep according to the Norton power-law

$$\dot{\epsilon}_e = \dot{\epsilon}(T)(\sigma_e/\sigma_0)^n \quad (5)$$

if not damaged. Here, n is the creep exponent, σ_0 a reference stress parameter, σ_e the effective Mises stress and $\dot{\epsilon}(T)$ the temperature dependent reference strain rate. The temperature dependence of $\dot{\epsilon}$ is taken in accordance with a standard Arrhenius law in terms of a reference strain rate $\dot{\epsilon}_0$ at the reference temperature T_0 .

Damage is described in terms of a continuous field of the (microscopic) damage parameters: average cavity radius a and average cavity spacing b . At each material point, a damage tensor is constructed from three principal values of a and b on families of grain facets that are approximately normal to the three principal macroscopic stress directions. The key quantity that governs the contribution of damage to the macroscopic inelastic deformation is the average separation between adjacent grains, $\delta = V^{cav}/(\pi b^2)$. Growth of the cavities occurs by a coupled process of creep of the grains and grain boundary diffusion. Accordingly, the final volumetric growth rate \dot{V}^{cav} can be written on the form

$$\dot{V}^{cav} = \dot{V}_{diff}^{cav}(a, b, p_m, \sigma_n, \sigma_e) + \dot{V}_{cr}^{cav}(a, b, p_m, \sigma_m, \sigma_e) \quad (6)$$

where $p_m = p_{CH_4} + p_{H_2}$ is the total gas pressure inside the cavity. Furthermore, σ_n is the normal stress on the grain boundary facet, σ_m the hydrostatic stress component and σ_e the effective Mises stress, all at a local scale near the cavity. The creep contribution \dot{V}_{cr}^{cav} depends on the creep properties appearing in (5), while the diffusive contribution \dot{V}_{diff}^{cav} depends on a temperature dependent grain boundary diffusion parameter \mathcal{D} as well as on the creep parameters.

The contribution of cavity growth to the macroscopic strain rate, through the grain boundary cavitation rate $\dot{\delta}$, depends on the mode of cavitation. If creep of the grains can

be neglected compared to the cavitation rate, the so-called rigid-grain mode is active. This results in a macroscopic dilatation which is a function of grain size. If creep cannot be neglected, the contribution to the macroscopic inelastic strain rate is based on a so-called penny-shaped crack model. This yields a dilatation, associated with void growth, as well as deviatoric components due to the reduced creep resistance of material with damaged grain facets. A criterion of maximum cavitation rate is adopted to select the mode of cavitation at each stage of the attack process.

RESULTS AND DISCUSSION

We analyse the decarburization and the hydrogen attack evolution in a 2.25Cr-1Mo pressure vessel with an internal radius of $r_i = 1.62$ m and an outer radius of $r_o = 1.72$ m. The operating conditions, being the temperature, the absolute pressure and the partial hydrogen pressure inside the vessel, are $T_i = 733$ K, $p = 14.3$ MPa and $p_{H_2,i} = 12.8$ MPa, respectively. We assume that the temperature at the outer surface of the vessel is $T_o = 723$ K and that steady state conditions occur which allow us to compute the radial distribution of the temperature $T(r)$ and the hydrogen pressure $p_{H_2}(r)$ [5].

The material parameters for 2.25Cr-1Mo steel are summarized in [5]. For the sake of brevity we will only discuss the creep data. The creep parameters of 2.25Cr-1Mo in (5) are determined by Klueh [3] who performed creep tests on 2.25Cr-1Mo steels with 0.009, 0.030, 0.12, and 0.135 wt% C at 454°C, 510°C, and 565°C. We can reproduce the measured creep rates of 2.25Cr-1Mo steels with different wt% C by assuming a linear dependence of σ_0 on the logarithm of c_c , $\sigma_0(c_c) = 985.7 + 170.9 \log c_c$ [MPa], while the other parameters are kept constant: $n = 8.5$ and $\dot{\epsilon}_0 = 5.5 \times 10^{-8} \text{s}^{-1}$ at $T_0 = 727$ K. Since only the ratio $B_0 = \dot{\epsilon}_0/\sigma_0^n$ is relevant, Figure 1 shows the used dependence of B_0 on c_c normalized by $B_0^{\text{norm}} = B_0(c_c = 0.15 \text{wt}\%)$. The dashed-dotted line signifies the region where we extrapolated ($c_c < 0.009 \text{wt}\%$) by using the described function $\sigma_0(c_c)$ until values for B_0 are reached which are comparable to the creep data of a pure α -Fe given in [6].

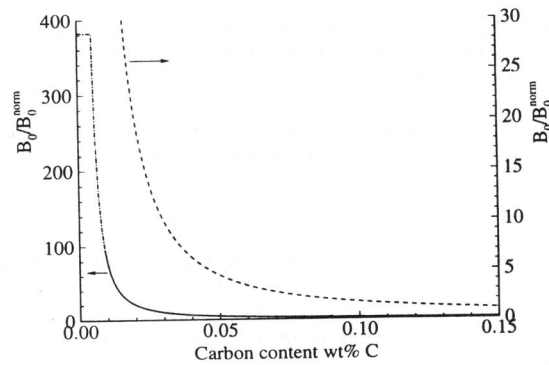


Figure 1: Dependence of $B_0 (= \dot{\epsilon}_0/\sigma_0^n)$ on the carbon content c_c , normalized by the value B_0^{norm} at $c_c = 0.15 \text{wt}\%$. The dashed line is a blow-up of the bottom regime.

A typical 2.25Cr-1Mo steel contains 0.15wt% C and M_7C_3 carbides with 60% Cr and 40% Fe. The calculated cavity pressure distribution under the operating conditions described above is shown in Figure 2. Also shown, are the corresponding carbon concentration profiles across the wall thickness at two stages of the lifetime, namely at $a/b = 0.4$ and at $a/b = 0.7$. No lower limits for the carbon content are given in the 2.25Cr-1Mo specification. Therefore, the initial carbon concentration could also be equal to 0.04 wt% C, where according to Figure 1 decarburization has a larger effect on the creep parameters. The carbon concentration profiles at $a/b = 0.4$ and at $a/b = 0.7$ are also shown in Figure 2.

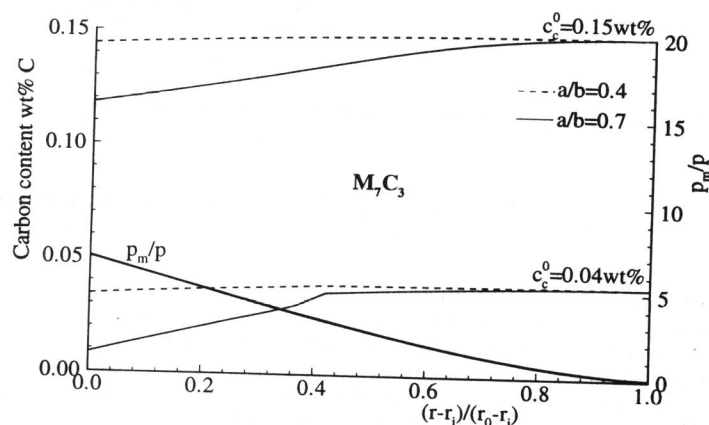


Figure 2: Distribution of the cavity pressure p_m and decarburization along the wall thickness for steels containing the carbide $(Cr_{0.6}Fe_{0.4})_7C_3$ with different initial carbon contents c_c^0 .

If the steel contains the more unstable carbide M_3C , the cavity pressure is much higher which results in a bigger difference between the carbon content at the inner surface and the outer surface of the vessel (see Figure 3).

Table 1 summarizes the failure times calculated for the previously discussed cases. We repeated the calculations by sticking to the initial creep parameter $B_0(c_c^0)$. This results in failure times given in the second line of Table 1. It turns out that the influence of decarburization on the total life time is rather small.

TABLE 1: Failure times in years of steels with different initial carbon contents c_c^0 and carbide types (M_7C_3 , M_3C).

$c_c^0 =$	$(Cr_{0.6}Fe_{0.4})_7C_3$		$(Cr_{0.3}Fe_{0.7})_3C$	
	0.15 wt% C	0.04 wt% C	0.15 wt% C	0.04 wt% C
with decarb.	27.96 years	24.63 years	12.73 years	10.27 years
w/o decarb.	28.00 years	24.97 years	12.82 years	11.32 years

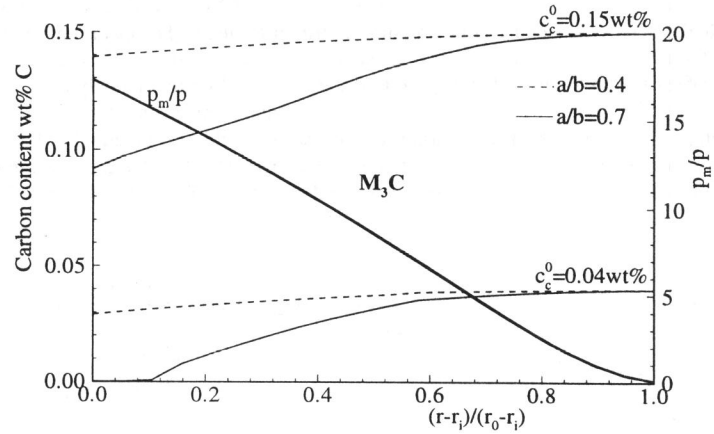


Figure 3: Distribution of the cavity pressure p_m and decarburization along the wall thickness for steels containing the carbide $(Cr_{0.3}Fe_{0.6})_3C$ with different initial carbon contents c_c^0 .

We conclude that the carbon content in a pressure vessel only deviates significantly from its initial value near the end of the failure time. Then, the difference in carbon concentration, that occurs for example in a vessel made of 2.25Cr-1Mo steel with a common microstructure between its inner and outer surface, is about 0.03wt% C (see Figure 2). This difference is too small to affect the mechanical behaviour because the creep parameters of a 2.25Cr-1Mo steel with 0.05wt% C differ from one with 0.15wt% C only by a factor 5 (Figure 1).

REFERENCES

- [1] Van der Burg, M.W.D., Van der Giessen, E. and Brouwer, R.C., *Acta Mat.*, Vol. 44, 1996, pp. 505-518.
- [2] Odette, G.R. and Vagarali, S.S., *Metall. Trans.*, Vol. 13A, 1982, pp. 299-303.
- [3] Klueh, R.L., *J. Nucl. Mater.*, Vol. 54, 1974, pp. 41-51.
- [4] Van der Burg, M.W.D. and Van der Giessen, E., *Acta mater.*, Vol. 45, 1997, pp. 3047-3057.
- [5] Van der Burg, M.W.D., Van der Giessen, E. and Tvergaard, V., *Mat. Sci. and Eng. A*, Vol. 241, 1998, pp. 1-13.
- [6] Frost, H.J. and Ashby, M.F., "Deformation-mechanism maps", Pergamon Press, Oxford, Great Britain, 1982.